Journal of Cellular Biochemistry 75:492–504 (1999)

αvβ3, αvβ5, and Osteopontin Are Coordinately Upregulated at Early Time Points in a Rabbit Model of Neointima Formation

Martha H. Corjay,* Sheila M. Diamond, Karen L. Schlingmann, Sandra K. Gibbs, Janet K. Stoltenborg, and Adrienne L. Racanelli

DuPont Pharmaceuticals Research Laboratories, Experimental Station, Wilmington, Delaware

Abstract Abstract Both smooth muscle cell migration and replication are known to be responsible for neointima formation. Recent reports based on in vitro studies and animal models of neointima formation highlight the possible importance of αvβ3 and αvβ5 integrins in mediating neointima formation. Clinical data suggest that specific αvβ3 blockade may limit restenosis. The aim of this study was to identify the expression of αvβ3 and αvβ5 and their ligand osteopontin in the very early phases of neointima formation in a rabbit model. A non-occlusive cuff placed around the rabbit femoral artery resulted in a complete, concentric neointima that formed by 14 days. Antibodies specific for the integrin heterodimers and for osteopontin, along with a probe specific for osteopontin mRNA, were used to identify expression at early time points (6 h, 1 day, 3 days, 5 days) post-cuffing. Immunohistochemistry and in situ hybridization expression results were quantitated by image analysis and tested for statistical significance by a two-tailed *t*-test. The data demonstrated the rapid (within 6 h) and abundant upregulation of αvβ3 and αvβ5 integrins and their ligand during very early time points of neointima formation. The very early (6 h) upregulation of αvβ3 underscores a potentially important clinical intervention point in limiting restenosis following clinical angioplasty procedures. J. Cell. Biochem. 75:492–504, 1999.

Key words: integrins; αvβ3; αvβ5; osteopontin; neointima formation; restenosis models

Neointima formation, a complex process involving smooth muscle cell adhesion, migration, and proliferation, commonly occurs following injury to blood vessels and is associated with both atherosclerotic and restenotic vascular lesions. Approximately 30% of patients develop significant coronary restenosis within 4 to 6 months of successful PTCA [Serruys et al., 1988; Nobuyoshi et al., 1988]. Since the etiologic cellular mechanisms of human restenosis are unknown, the area is the subject of intense investigation. Cell culture studies focusing on vascular smooth muscle cell (SMC) adhesion and migration have implicated a critical role for integrin heterodimers in mediating cell-matrix interactions and smooth muscle cell migration Brown et al., 1994; Jones et al., 1996; Liaw et al., 1995a]. Osteopontin, a ligand for αvβ3, αvβ5, and αvβ1, has been shown to specifically support SMC adhesion to all three integrins and to mediate SMC migration specifically via the αvβ3 receptor [Liaw et al., 1995a]. In view of the possible importance these cellular receptors may have in pathological processes, recent efforts have been directed towards examining in vivo vascular expression and distribution of integrins. αvβ3, αvβ5, and osteopontin are all known to be expressed by vascular SMC [Liaw et al., 1995a; Giachelli et al., 1995]. αvβ3 is widely expressed throughout normal vasculature [Corjay et al., 1996; Hoshiga et al., 1995]. In addition, αvβ3 is expressed in human atherosclerotic arteries [Hoshiga et al., 1995] and its ligand osteopontin has been shown to be upregulated in human atherosclerotic and restenotic lesions as well as in animal models of neointima formation [Giachelli et al., 1993; O'Brien et al., 1994; Hirota et al., 1993; Shanahan et al., 1993].

The potential role of integrins in the process of intimal thickening is suggested by clinical pharmacological intervention studies. Data

*Correspondence to: Martha H. Corjay, DuPont Pharmaceuticals Research Laboratories, Experimental Station, Route 141, E400/3227, Wilmington, DE 19880-0400. E-mail: martha.h.corjay@dupontpharma.com

Received 16 February 1999; Accepted 30 April 1999

from the EPIC trial suggest that blockade of β3 activity, specifically αIIbβ3 and αvβ3, significantly reduces post-angioplasty restenosis [Topol et al., 1994]. Subsequent clinical studies with antagonists specific for αIIbβ3 failed to limit restenosis, indicating that the therapeutic effect of ReoPro may be due to specific αvβ3 blockade [Lincoff et al., 1995]. In addition, RGD-antagonists have been shown to inhibit neointima formation in rabbit and hamster injury models [Choi et al., 1994; Matsuno et al., 1994]. Specific αvβ3 antagonists have been shown to limit vascular neointima formation in porcine and guinea pig injury models [Srivatsa et al., 1997; Le Breton et al., 1996]. Neutralizing antibodies to osteopontin have been shown to limit neointimal thickening in rat carotid artery following balloon catheterization [Liaw et al., 1997]. Taken together, these data underscore a potential functional role for integrin and osteopontin mediated cell adhesion and migration in the neointima growth process.

The process of neointima formation has been investigated using animal models employing either intraluminal or perivascular injury to blood vessels [De Meyer et al., 1991, 1997; Kockx et al., 1992, 1993]. Previously published reports have shown that placement of a nonconstrictive, flexible cuff around the rabbit carotid artery results in neointima formation. In this model, a superficial injury is produced and characterized by small foci of endothelial denudation at 6 h that is followed by complete reendothelialization by 24 h [Kockx et al., 1992, 1993]. It has been demonstrated that SMC replication in the media precedes neointimal formation at 2 weeks [Kockx et al., 1992]. This model has been well characterized by histopathologic methods, making it suitable for the study of SMC replication, migration, and neointima formation [Kockx et al., 1992, 1993]. The aim of the present study was to investigate the spatial and temporal regulation of αvβ3, αvβ5, and osteopontin at early time points in a rabbit perivascular injury model of neointima formation. A non-occlusive cuff was placed around the rabbit femoral artery, which resulted in maximal SMC proliferation at 3 to 5 days post-injury. A complete, concentric neointima formed by 14 days. The data presented here demonstrate a rapid (within 6 h post-cuffing) and abundant upregulation of αvβ3 and αvβ5 integrins and their ligand osteopontin. The upregulation exhibits a specific temporal and spatial expression pattern, suggesting that αvβ3 and αvβ5 integrins and their ligand osteopontin together may play a functional role in mediating SMC adhesion and migration leading to neointima formation.

MATERIALS AND METHODS

Experimental Design

Male New Zealand rabbits (2.2 to 2.7 kg) were anesthetized with Ketamine® (40 mg/kg i.m.), Xylazine® (5 mg/kg i.m.) and isoflurane maintenance. Femoral arteries were surgically exposed using aseptic techniques and a nonocclusive, flexible silicone cuff (Cole-Parmer, Vernon Hills, IL; 1 cm in length, 1.6 mm internal diameter, 0.8 mm wall thickness) was placed around the left femoral artery [Kockx et al., 1992, 1993]. The centrally acting analgesic Nubain® (2 mg/kg, s.c.) was administered postoperatively. Five animals with uncuffed arteries were evaluated for integrin and osteopontin expression, and five animals were evaluated for integrin and osteopontin expression at each of the following time points after cuff placement: 6 h, 1 day, 3 days, and 5 days. At 2 weeks, five animals were evaluated for neointima formation. Rabbits were anesthetized with Ketamine® (80 mg/kg i.m.), Xylazine® (10 mg/kg i.m.), and Nembutal® (20 mg/kg i.v.). The vasculature was flushed with PBS prior to perfusion fixation with 4% paraformaldehyde. The cuff was isolated from the femoral artery, and the area of the cuffed region was immersion fixed for 4 h in 4% paraformaldehyde, dehydrated, cleared, and infiltrated with paraffin in a Tissue-Tek II automatic tissue processor (Sakura Finetechnical, Tokyo, Japan). Prior to tissue embedding, the artery was transected at the center point of the cuff. Sections (4 μM) were cut and mounted on Superfrost Plus microscope slides (VWR Scientific, Bridgeport, NJ). Animal studies were approved by the DuPont Pharmaceuticals Research Laboratories Institutional Committee for the Care and Use of Animals and the investigation conforms with the *Guide for the Care and Use of Laboratory Animals* published by the US National Institutes of Health (NIH publication No. 85–23, revised l996).

Paraffin-embedded human multi-tissue slides were obtained from Dako Corporation (Carpinteria, CA).

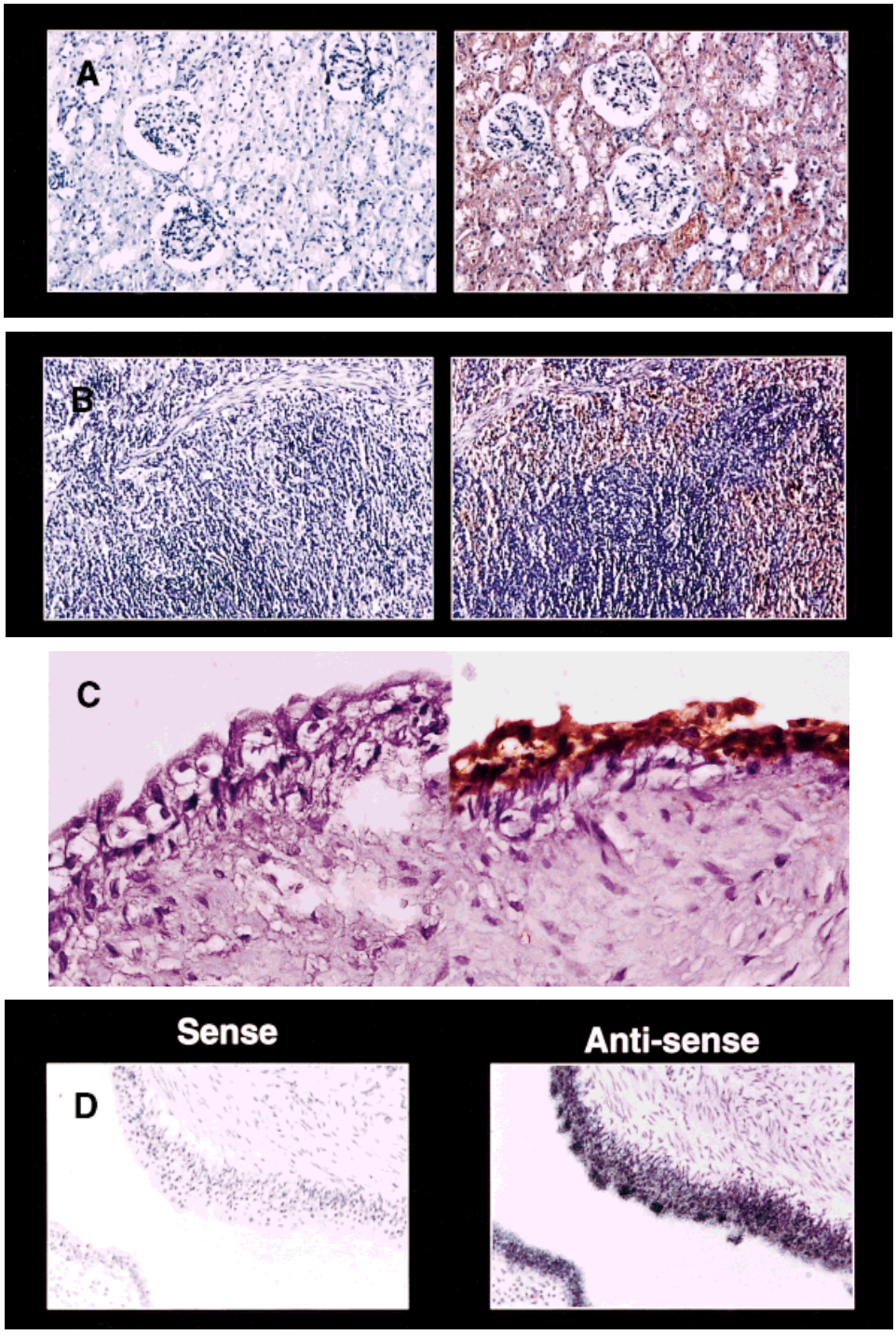

Fig. 1. Specificity of antibodies and in situ hybridization probe. **A:** Rabbit kidney stained with anti-αvβ3 monoclonal antibody (**right**) or with an isotype matched monoclonal control antibody (**left**). **B:** Rabbit spleen stained with anti-αvβ5 monoclonal antibody (**right**) or with an isotype matched monoclonal control antibody (**left**). **C:** Rabbit kidney stained with guinea pig anti-osteopontin antiserum (**right**) or with antigen-depleted antiserum (**left**). **D:** Rabbit kidney hybridized with osteopontin anti-sense probe (**right**) or with control sense probe (**left**). **E:** Western blot of rabbit kidney extract run on a native gel and probed with the anti-αvβ3 monoclonal, HB4; rabbit spleen extract probed with the anti-αvβ5 monoclonal, P1F6; and rabbit kidney extract probed with the polyclonal anti-osteopontin serum.

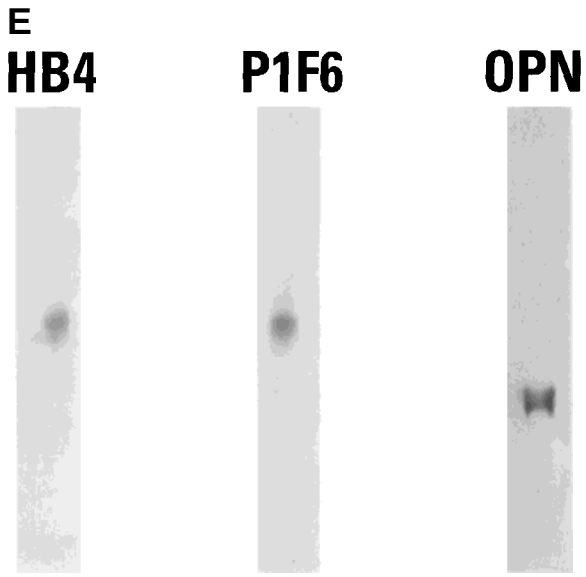

Figure 1. (Continued.)

Western Blot Analysis

Excised tissue was rinsed in cold phosphate-buffered saline, weighed and diced in phosphate buffered saline containing 100 mM n-octylglucoside (Calbiochem, San Diego, CA), 5 mM PMSF, 10 mg/ml benzamidine, and 1 U/ml aprotinin. Solubilization for 1 h at room temperature was followed by freeze/thaw and centrifugation at 14,000*g* at 4°C. Protein concentrations of samples were determined using a micro-BCA assay (Pierce Chemical Company, Rockford, IL). Samples were diluted 1:2 in Seprasol without β-mercaptoethanol (Integrated Separations Systems, Natick, MA) and 750 µg total protein loaded per lane. Samples were run on 10–18% gradient gels and transferred overnight onto PVDF membrane. Blots were blocked with 0.5% I-block (Tropix, Bedford, MA) and were subsequently incubated with anti-αvβ3 monoclonal antibody, HB4 (15 µg/ml); anti-αvβ5 monoclonal antibody, P1F6 (15 µg/ml) or with anti-osteopontin antisera (1:500) overnight at 4°C. Following washes in Tris pH 7.4, containing 0.05% Tween 20, blots were incubated with secondary antibody for 2 h at room temperature. Blots were developed using CPD Star Chemiluminescence (Tropix). Exposure was for 30 to 60 s.

Immunohistochemistry

The monoclonal antibody specific for the αvβ5 complex, clone P1F6, was purchased from Becton Dickinson (San Jose, CA) and used at 15 µg/ml [Smith et al., 1990]. Clone P1F6, raised against human αvβ5, has been shown to cross-react with rabbit αvβ5 [Friedlander et al., 1995]. However, the specificity of this reaction was confirmed by Western blotting (Fig. 1E). Staining was demonstrated to be mediated by antigen recognition, as incubation of a isotype matched antibody that recognizes a protein neither expressed or inducible in mammalian cells, demonstrated no staining (Fig. 1B). The monoclonal antibody HB4 was raised against the αvβ3 integrin purified from human placental tissue. This antibody was shown to recognize the intact rabbit αvβ3 complex by Western blot (Fig. 1E) and to inhibit osteopontin-mediated migration of human smooth muscle cells [Walton et al., 1996]. In addition, HB4 was shown to react with αvβ3 receptors on human 293 cells transfected with an αvβ3 expressing construct, whereas the αvβ3 negative parent cell line demonstrated no reactivity with the antibody [Walton et al., 1996]. Both HB4 and the prototypical αvβ3 antibody LM609 (Chemicon, Temecula, CA) were shown to have the identical, previously reported characteristic staining pattern on rabbit kidney (Fig. 1A) [Rabb et al., 1996]. HB4 was diluted to an optimum concentration of 1.25 µg/ml and LM609 was used at 15 µg/ml. Serial sections of rabbit femoral artery were immunostained with both αvβ3 specific antibodies, yielding identical results. A polyclonal antibody was raised in guinea pig against human osteopontin and was delipidated and filter sterilized before immunostaining. Antibody specificity for osteopontin was demonstrated by Western blotting (Fig. 1E) and by affinity depletion of osteopontin-specific antibodies from the polyclonal antisera, which effectively eliminated staining (Fig. 1C). When diluted 1/1,000, the osteopontin polyclonal antibody demonstrated specificity for osteopontin present on luminal epithelial surfaces in human tissues and rabbit kidney [Brown et al., 1992; Lopez et al., 1993]. Controls were diluted to the same concentration as the corresponding primary antibodies and included IgG isotype clone DAK-GO1(IgG1, Dako) for the monoclonal antibodies and preimmune sera for the polyclonal antibody. The study was designed such that serial sections were evaluated with each specific antibody and its corresponding control, with each done in triplicate. In addition, adjacent sections were

used to compare integrin and osteopontin expression.

Immunostaining was performed by an indirect peroxidase antibody conjugate method using the Vectastain ABC Elite (Vector Laboratories, Burlingame, CA) peroxidase system with a DAB substrate. Primary antibody was incubated on sections at 4° C overnight, the sections were incubated with secondary and conjugated antibodies according to the manufacturer's instructions, and DAB substrate was applied to detect positive immunostaining. Slides were rinsed with distilled water and counterstained lightly with Harris hematoxylin using a regressive method.

In Situ Hybridization

A synthetic oligonucleotide probe complementary to bases 204 to 247 of rabbit osteopontin cDNA [Tezuka et al., 1992] and to bases 229 to 272 of human osteopontin cDNA [Kiefer et al., 1989] was shown to be specific for osteopontin mRNA in rabbit kidney and human epithelial cells, whereas the sense probe from the same region did not hybridize (Fig. 1D). The probe is from regions of 100% homology between rabbit and human osteopontin and did not exhibit complementarity to other sequences in the gene data base. Rabbit tissues for in situ hybridization were processed as described above for immunohistochemistry, with precautions taken to ensure RNase-free conditions. The enzyme 3′-Terminal deoxynucleotidyl transferase (Promega, Madison, WI) was used to label sense and anti-sense probes with S-dATP. In situ hybridization was performed as previously described [Wilcox, 1993]. Briefly, paraffin-embedded tissues were deparaffinized, fixed in 4% paraformaldehyde, pH 7.4, at 4°C for 10 min, pretreated with proteinase K at 1 μg/ml, and prehybridized in hybridization buffer (10 mM DTT, 1 × Denhardt's, 5 × SSC, 100 μg/ml salmon sperm DNA, 100 μg/ml tRNA, 10% dextran sulfate, 20% formamide) for 1 to 3 h at room temperature. Hybridization buffer containing 300,000 cpm of ^{35}S-labeled sense and antisense probes was added to prehybridized tissue sections and hybridization was performed overnight at 42°C. Slides were washed with 2 × SSC containing 10 mM β-mercaptoethanol and 1 mM EDTA at room temperature. Slides were washed in a high stringency wash of 0.1 × SSC with 10 mM β-mercaptoethanol and 1 mM EDTA for 2 h at 47°C. Slides were washed with 0.1 × SSC and dehydrated in graded alcohols containing 0.3 M ammonium acetate. Slides were dried, coated with NTB2 nuclear track emulsion (Eastman Kodak Co., New Haven, CT), and exposed in the dark at 4°C for 6 weeks. After development, slides were counterstained with hematoxylin and eosin.

Analysis of Results

Five rabbits with uncuffed femorals and five rabbits with cuffed femorals were analyzed at each time point post-cuffing (6 h, 1 day, 3 days, and 5 days) for αvβ3, αvβ5, and osteopontin protein expression by immunohistochemistry and analyzed for osteopontin mRNA by in situ hybridization. Each femoral was cut at the midpoint of cuff location and embedded so that three sections per specimen were analyzed for each protein and mRNA. Therefore, fifteen sections in total were analyzed for the expression level of each molecule at each time point. An Olympus microscope linked to a MicroComputer Imaging Device (MCID) M4 system (Ontario, Canada) equipped with a DAGE-MTI model 72S solid state CCD camera was used to capture and quantitate images. In order to eliminate the counting of nuclei (hematoxylin stained) or eosin-stained cytoplasm, density levels greater than a threshold level were measured as corresponding to DAB substrate, indicating positive immunoreactivity. All immunohistochemistry samples were analyzed using the same shading correction and density threshold. Rather than calibrating density levels to a standard stained tissue, data are reported as density per unit area. Results of in situ hybridization were quantitated by automated grain counting of the DAGE camera-captured images. Results are reported as grain pixels per total area pixels.

RESULTS

The objective of the study was to examine the early expression of αvβ3 and αvβ5 integrins and their ligand, osteopontin, in a rabbit model of neointima formation. The specificity of the antibodies and in situ hybridization probe used in this study is shown in Figure 1. The concentric neointima that formed by 2 weeks after placement of the non-occlusive cuff around the femoral artery is demonstrated in Figure 2. The neointima formation was preceded by prolifera-

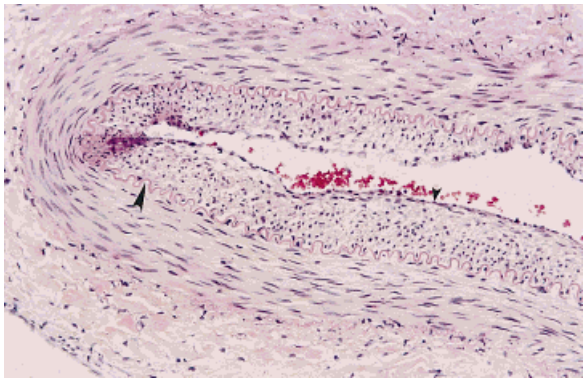

Fig. 2. Neointima formation after cuffing the femoral artery. A complete, concentric neointima was formed by 2 weeks following the placement of a non-occlusive cuff around the rabbit femoral artery. Vessels were fixed in 4% paraformaldehyde, paraffin embedded, cut into 4 μM sections, and counterstained with Harris' hematoxylin and eosin. The small arrowhead points to neointima; the large arrowhead points to internal elastic lamina. Original magnification, ×200.

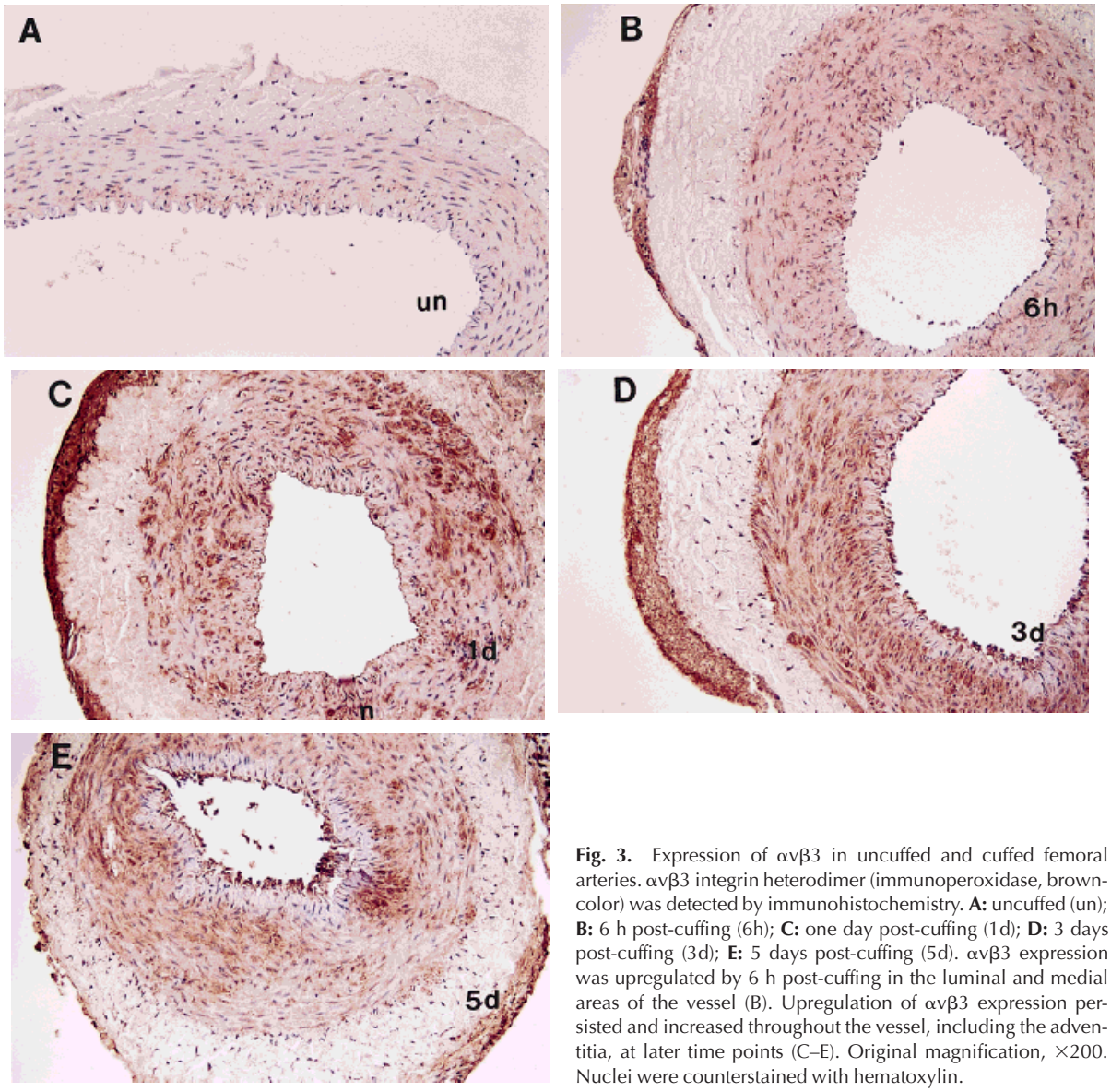

Fig. 3. Expression of αvβ3 in uncuffed and cuffed femoral arteries. αvβ3 integrin heterodimer (immunoperoxidase, brown-color) was detected by immunohistochemistry. **A:** uncuffed (un); **B:** 6 h post-cuffing (6h); **C:** one day post-cuffing (1d); **D:** 3 days post-cuffing (3d); **E:** 5 days post-cuffing (5d). αvβ3 expression was upregulated by 6 h post-cuffing in the luminal and medial areas of the vessel (B). Upregulation of αvβ3 expression persisted and increased throughout the vessel, including the adventitia, at later time points (C–E). Original magnification, ×200. Nuclei were counterstained with hematoxylin.

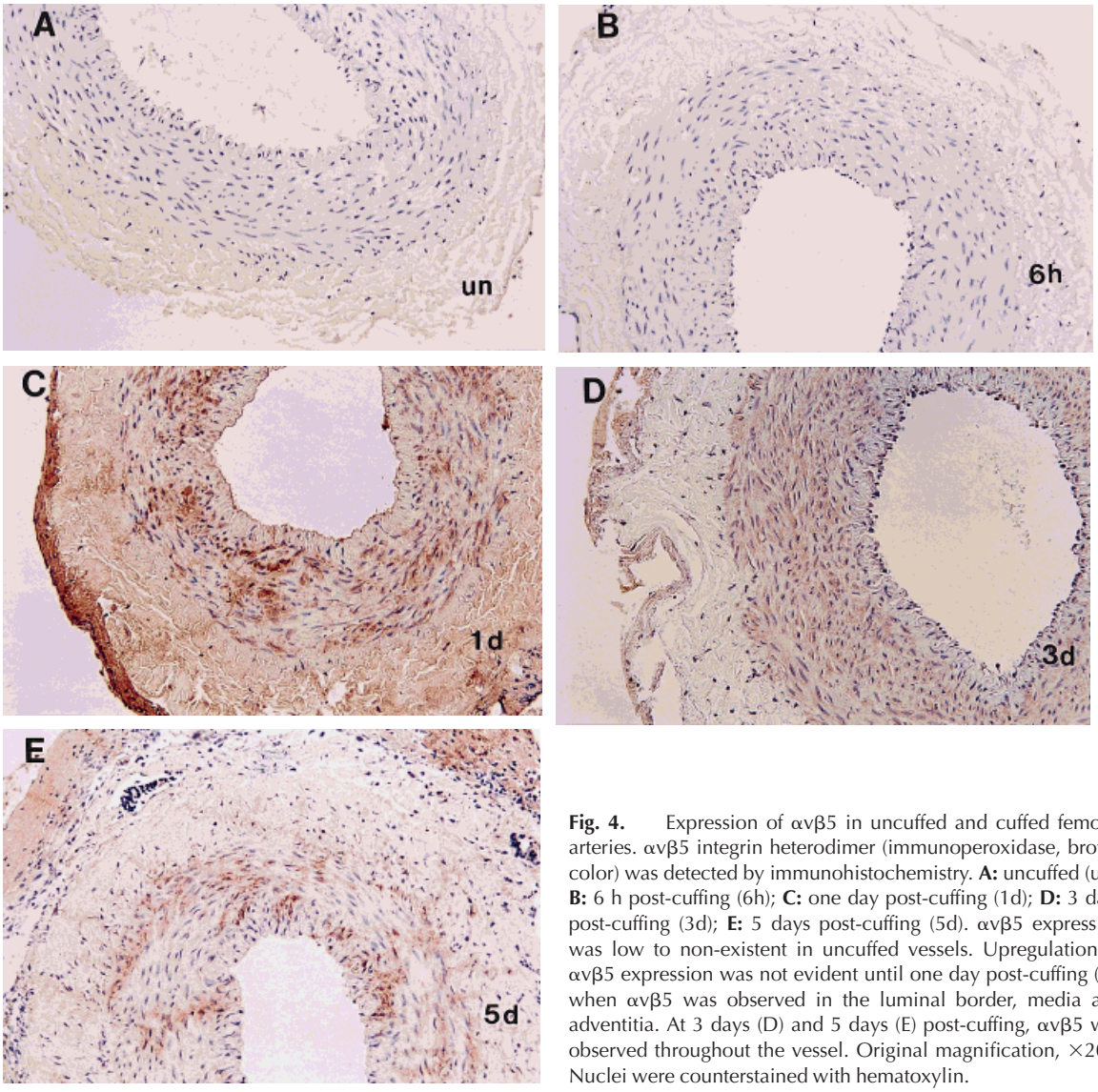

Fig. 4. Expression of αvβ5 in uncuffed and cuffed femoral arteries. αvβ5 integrin heterodimer (immunoperoxidase, brown color) was detected by immunohistochemistry. **A:** uncuffed (un); **B:** 6 h post-cuffing (6h); **C:** one day post-cuffing (1d); **D:** 3 days post-cuffing (3d); **E:** 5 days post-cuffing (5d). αvβ5 expression was low to non-existent in uncuffed vessels. Upregulation of αvβ5 expression was not evident until one day post-cuffing (C), when αvβ5 was observed in the luminal border, media and adventitia. At 3 days (D) and 5 days (E) post-cuffing, αvβ5 was observed throughout the vessel. Original magnification, ×200. Nuclei were counterstained with hematoxylin.

tion that occurred maximally between days 3 and 5 post-cuffing, as determined by bromodeoxyuridine incorporation (data not shown). Although cuffing resulted in neointima formation, sham-operated vessels did not form a neointima (data not shown). These data are consistent with previously published results in this model of neointima formation [Kockx et al., 1992, 1993].

Expression of αvβ3 integrin in normal rabbit femoral artery and at 6 h, 1 day, 3 days, and 5 days post-cuffing is shown in Figure 3. Basal expression of αvβ3 in normal rabbit femoral artery was shown to be low (Fig. 3A). At 6 h post-cuffing, αvβ3 expression was upregulated in the luminal and medial areas (Fig. 3B). At one day post-cuffing (Fig. 3C), αvβ3 upregulation increased in the luminal and medial areas, where the expression was characterized by a distinct mottled appearance. At one day, adventitial upregulation was also noted. At 3 and 5 days post-cuffing (Fig. 3D and E), αvβ3 expression was maintained at high levels throughout the vessel, with significant upregulation in the media and along the extreme luminal periphery of the femoral artery, the luminal border.

Expression of αvβ5 integrin was evaluated in sections adjacent to those analyzed for αvβ3 expression (Fig. 4). Expression of αvβ5 integrin was extremely low to non-existent in normal, control femoral arteries (Fig. 4A). Observable changes post-cuffing did not occur until day one, when significant upregulation was detected in

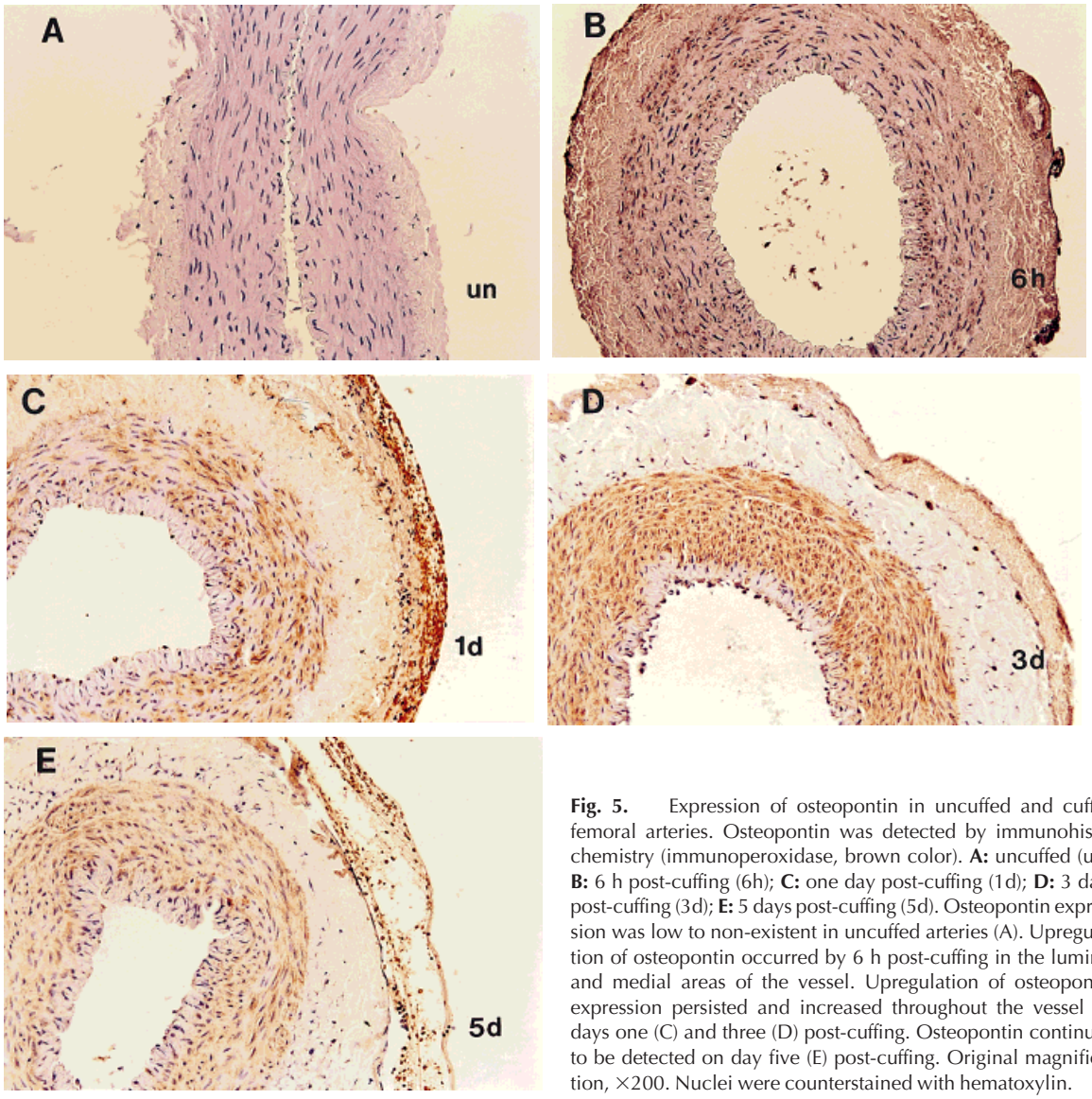

Fig. 5. Expression of osteopontin in uncuffed and cuffed femoral arteries. Osteopontin was detected by immunohistochemistry (immunoperoxidase, brown color). **A:** uncuffed (un); **B:** 6 h post-cuffing (6h); **C:** one day post-cuffing (1d); **D:** 3 days post-cuffing (3d); **E:** 5 days post-cuffing (5d). Osteopontin expression was low to non-existent in uncuffed arteries (A). Upregulation of osteopontin occurred by 6 h post-cuffing in the luminal and medial areas of the vessel. Upregulation of osteopontin expression persisted and increased throughout the vessel on days one (C) and three (D) post-cuffing. Osteopontin continued to be detected on day five (E) post-cuffing. Original magnification, ×200. Nuclei were counterstained with hematoxylin.

patches throughout the artery (Fig. 4C). By 3 days post-cuffing, αvβ5 expression was observed to be more diffuse than at one day, and was detected throughout the vessel (Fig. 4D). By 5 days post-cuffing, αvβ5 was confined to a more limited area of the vessel (Fig. 4E). Overall, αvβ5 expression was distributed in a more mottled pattern than was αvβ3 expression.

While the uninjured artery demonstrated little or no osteopontin expression (Fig. 5A), osteopontin was upregulated in the media and interior periphery of the artery as early as six hours post-cuffing (Fig. 5B). Expression of osteopontin in the medial area at one day was mottled (Fig. 5C), while by day 3 osteopontin immunostaining was more widely dispersed throughout the medial area. In the adventitia, osteopontin expression was detected at one day post-cuffing and upregulated levels were maintained through the 5-day post-cuffing period.

Although representative photomicrographs are shown here, in order to thoroughly analyze results from all five animals at each time point, quantitative densitometric analysis was performed with the MCID M4 Image Analysis System. These results were then subjected to statistical analysis comparing expression levels of each protein within a particular region of the arterial cross-section. Specifically, expression was analyzed with respect to adventitial levels, medial levels, and the luminal adjacent border region and were subsequently tested for statis-

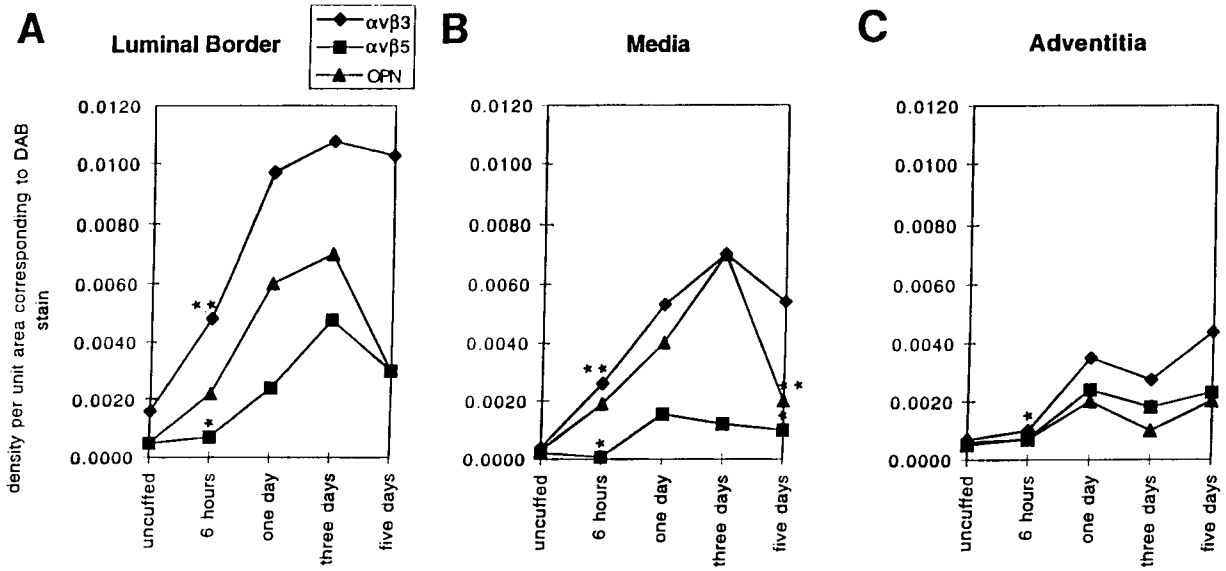

Fig. 6. Expression of αvβ3, αvβ5, and osteopontin in uncuffed femoral arteries and post-cuffing (see x-axis for time points) in the luminal border (**A**), media (**B**), and adventitia (**C**) as detected by immumohistochemistry and quantitated by the MCID M4 Image Analysis System. Density levels greater than a threshold level (to subtract away hematoxylin-stained nuclei) represent DAB substrate and correspond to positive immunohistochemistry. A standard shading correction and density threshold were applied to all analyses. Results were calculated as density per unit area (Y-axis). With respect to control uncuffed arteries, there was a statistically significant difference ($P < 0.05$, two-tailed *t*-test, N = 15 sections) for all expression levels post-cuffing, with three exceptions having a lower level of significance (**$P \leq 0.09$) and some levels at 6 h representing no difference from control (*$P > 0.5$). Overall, the greatest changes in integrin and osteopontin expression were observed in the medial area and luminal border region.

tical significance using a two-tailed *t*-test, N = 15. In order to compensate for slight variations in counterstaining, subtracted background readings were derived for each section separately. After analysis, integrin and osteopontin expression levels were plotted vs. time (Fig. 6). This analysis demonstrated that αvβ3 upregulation appeared by 6 h and peaked at 3 days both in the media and luminal border. Likewise, both αvβ5 and osteopontin levels peaked at 3 days.

Osteopontin mRNA expression as detected by in situ hybridization methods is shown in Figure 6. In normal, uninjured femoral arteries (Fig. 7A), osteopontin was highly expressed in the adventitia while little or no hybridization signal was evident in the luminal border and media. At 6 h post-cuffing, osteopontin mRNA was diffusely expressed throughout the media and persisted at high levels in the adventitia. Small foci of osteopontin mRNA were observed along the luminal border. By one day post-cuffing, prominent foci of osteopontin mRNA were noted in discrete areas along the luminal border, in the media, and in the adventitial region. In contrast, by 3 days the number of intense foci had diminished and signal for osteopontin mRNA was diffuse throughout the arterial cross-section. By day 5 post-cuffing, discrete foci of intense osteopontin mRNA expression were observed in conjunction with diffuse mRNA expression, particularly in the adventitia and luminal border regions. Quanititation of osteopontin mRNA expression by automated grain counting of DAGE captured images is shown in Figure 8. The highest level of osteopontin mRNA expression was observed in the adventitia. Notably, the level of osteopontin mRNA also peaked at 3 days post-cuffing.

DISCUSSION

This study reports the coordinated expression of αvβ3 and αvβ5 integrins and their ligand, osteopontin, in a rabbit model of neointima formation. Although this model is not likely to fully represent human restenosis, the processess that occur in the formation of neointima in this setting, such as cellular migration, are also likely to be involved in clinical restenosis. By the use of antibodies specific for αvβ3 and αvβ5 heterodimers and osteopontin, and an oligonucleotide probe specific for osteopontin, a temporal and spatial regulation of expression of these molecules during the very early time points (within 6 h) of neointima

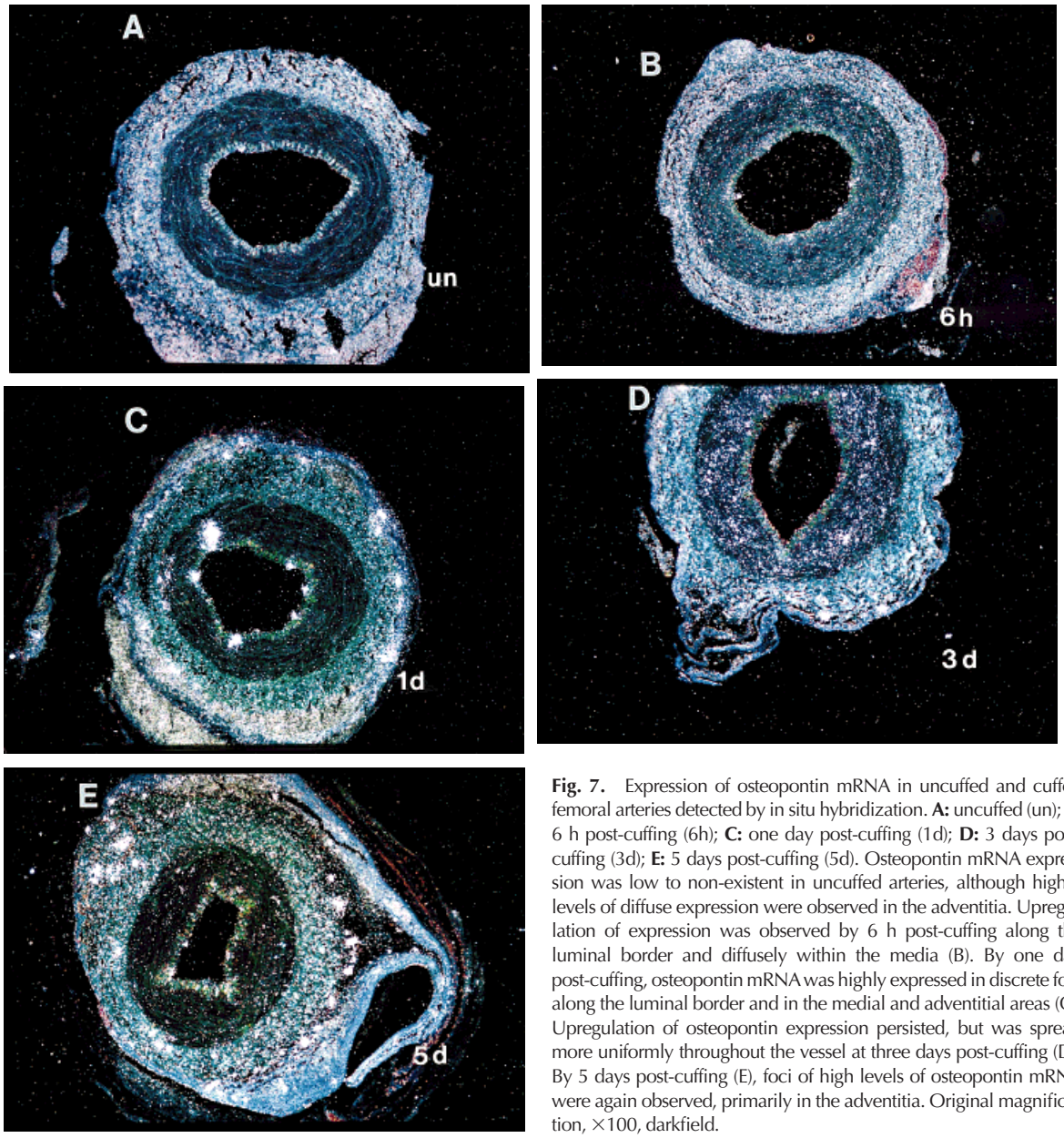

Fig. 7. Expression of osteopontin mRNA in uncuffed and cuffed femoral arteries detected by in situ hybridization. **A:** uncuffed (un); **B:** 6 h post-cuffing (6h); **C:** one day post-cuffing (1d); **D:** 3 days post-cuffing (3d); **E:** 5 days post-cuffing (5d). Osteopontin mRNA expression was low to non-existent in uncuffed arteries, although higher levels of diffuse expression were observed in the adventitia. Upregulation of expression was observed by 6 h post-cuffing along the luminal border and diffusely within the media (B). By one day post-cuffing, osteopontin mRNA was highly expressed in discrete foci along the luminal border and in the medial and adventitial areas (C). Upregulation of osteopontin expression persisted, but was spread more uniformly throughout the vessel at three days post-cuffing (D). By 5 days post-cuffing (E), foci of high levels of osteopontin mRNA were again observed, primarily in the adventitia. Original magnification, ×100, darkfield.

formation was observed. An additional significant obersvation in this study is the upregulation of αvβ3, αvβ5 and osteopontin followed by a later decrease in the level of expression. This study not only demonstrates the very early upregulation, but also by utilizing serial sections in the analysis, this study permitted an analysis of the relative spatial expression of each of the integrins and their ligand osteopontin relative to each other.

A previously published report on the cuffing injury model employed in these studies detailed three distinct phases that occur in neointima formation [Kockx et al., 1992]. First, minimal endothelial denudation is accompanied by increased endothelial permeability and a single wave of polymorphonuclear leukocyte infiltration, which peaks between 6 and 24 h. Next, medial SMC replication was reported to begin at 12 h and to diminish after 7 days. Finally, SMC accumulation in the subendothelial space is first observed at 3 days, and a concentric neointima is formed by 2 weeks. It was reported that sham-operated vessels did not produce a neointima, whereas cuffed vessels did. It was also previously reported that endothelial cells (ECs) in the cuffed vessel were altered morphologically and contained higher levels of von

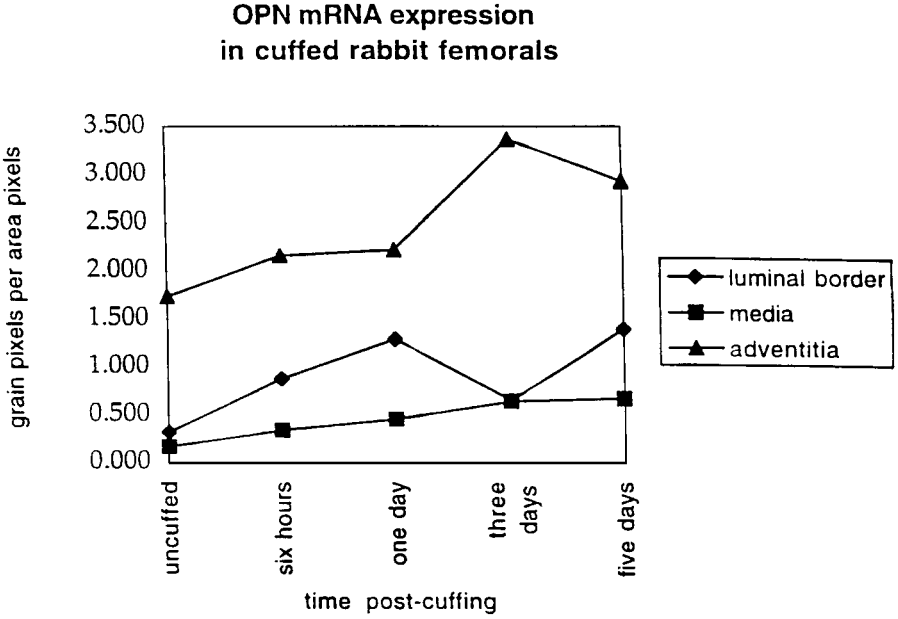

Fig. 8. Osteopontin mRNA expression in uncuffed and cuffed rabbit femoral arteries as measured by MCID M4 Analysis of DAGE captured images. Results were determined from automated grain counting per total area in the luminal border, media, and adventitia. Results are reported as grain pixels per area pixels.

Willebrand factor deposition [Kockx et al., 1993]. These data suggest that altered EC function contributes to increased adhesiveness and plays a role in neointima formation. Furthermore, minimal SMC damage was noted as a result of cuffing injury. A recent investigation demonstrates that the extent of neointimal thickening corresponds directly to the tightness of the collar around the artery [DeMeyer et al., 1997]. The authors suggest that interruption of transmural flow and trapping of cytokines within the cuffed segment contribute to the mechanism of neointima formation.

The data presented in this study demonstrated the specific elevation of osteopontin and integrin expression on the luminal border of the artery during the 6-h to 1-day time frame, the period when there may be increased permeability and the endothelium is regenerating. During the 3- to 5-day time interval, when SMC are proliferating and beginning to migrate, a dramatic increase in medial expression of $\alpha v\beta 3$, $\alpha v\beta 5$, and osteopontin was noted. At later time points (2 weeks, data not shown), integrin and osteopontin expression levels returned to levels approaching those observed in the uninjured state. Notably, at this later time point there is minimal SMC proliferation and little additional accumulation of neointima occurring. Accordingly, these data demonstrate a coordinated upregulation of $\alpha v\beta 3$, $\alpha v\beta 5$, and osteopontin as an early event preceding neointima formation. The specific localization of abundant osteopontin mRNA in the vessel wall indicated that this secreted protein was synthesized in the femoral artery itself, and was not produced in some other location. However, the expression of osteopontin mRNA in the adventitia of uninjured femorals, along with the lack of immunoreactivity in the uninjured vessel, indicate that the protein does not normally accumulate in the normal femoral.

In addition to integrins and their ligands, other factors have been implicated in the neointima growth process. The release of various chemoattractants, growth factors, and cytokines is associated with neointima formation [Liu et al., 1989; Ip et al., 1990]. Medial SMC have been shown to proliferate in response to the endogenous release of basic fibroblast growth factor (bFGF) by injured arterial cells [Lindner et al., 1990]. Additionally, bFGF and PDGF have been demonstrated to stimulate the migration of SMC in denuded arteries [Lindner et al., 1990; Jawien et al., 1992]. Furthermore, in vitro studies demonstrate a link between these factors and integrin and osteopontin expression. Three factors implicated in the rat arterial response to injury process, bFGF, TGF-β, and angiotensin II, all stimulate vascular SMC to produce osteopontin [Giachelli et al., 1993]. The growth factors, PDGF and TGF-β, induce $\beta 3$ expression in rabbit and bovine SMC in vitro [Janat et al., 1992; Basson et al., 1992].

The focus of this investigation, αvβ3, was chosen in view of the accumulating data suggesting that this integrin may be a critical mediator in restenosis and atherosclerosis [Topol et al., 1994; Lincoff et al., 1995; Choi et al., 1994; Matsuno et al., 1994; Srivatsa et al., 1997; Le Breton et al., 1996]. A ligand for αvβ3, osteopontin, has also been implicated as a potential mediator of restenosis and atherosclerosis [Liaw et al., 1997]. Although osteopontin has been shown to interact with at least three integrin receptors, αvβ3, αvβ5, and αvβ1, it was not possible to evaluate αvβ1 in this investigation because there are no αvβ1 heterodimer specific probes or antibodies available at this time. The decision to focus on αvβ3 stems from reports on its unique role with osteopontin in mediating smooth muscle cell migration [Liaw et al., 1995a]. In addition, a recently published study has demonstrated a functional role for osteopontin in the process of neointimal thickening in vivo [Liaw et al., 1997]. Specifically, neutralizing antibodies to osteopontin significantly decreased both neointimal areas and cell numbers in a rat carotid artery model employing endothelial denudation via balloon catheterization.

These data confirm previously published reports and extend the original observations to include another species and another model of neointimal formation. In a rat balloon injury model, elevated osteopontin and β3 mRNA levels were observed at early time points and osteopontin protein levels were shown to parallel the time course of mRNA expression [Liaw et al., 1995b]. Other investigators used a rat aortic balloon injury model to demonstrate upregulated mRNA and protein expression of the integrin receptor subunits αv, β3, and β5 at early time points in the process of neointima formation [Graf et al., 1996]. The present investigation is the first to evaluate and identify the specific integrin heterodimers, αvβ3 and αvβ5, and both protein and mRNA expression of osteopontin, in the setting of neointima formation. As such, these data demonstrate the rapid increase in expression of osteopontin and two of its integrin receptors during the early time points of neointima formation, and suggest that their interaction may mediate adhesion and migration in the early phases of neointima formation.

REFERENCES

Basson CT, Kocher O, Basson MD, Asis A, Madri JA. 1992. Differential modulation of vascular cell integrin and extracellular matrix expression in vitro by TGF-β1 correlates with reciprocal effects on cell migration. J Cell Physiol 153:118–128.

Brown LF, Berse B, Van De Water L, Papadopoulos-Sergiou A, Perruzzi CA, Manseau EJ, Dvorak HF, Senger DR. 1992. Expression and distribution of osteopontin in human tissues: Widespread association with luminal epithelial surfaces. Mol Biol Cell 3:1169–1180.

Brown SL, Lundgren CH, Nordt T, Fujii S. 1994. Stimulation of migration of human aortic smooth muscle cells by vitronectin: implications for atherosclerosis. Cardiovasc Res 28:1815–1820.

Choi ET, Engel L, Callow AD, Sun S, Trachtenberg J, Santoro S, Ryan US. 1994. Inhibition of neointimal hyperplasia by blocking alpha V beta 3 integrin with a small peptide antagonist GpenGRGDSPCA. J Vasc Surg 19: 125–134.

Corjay MH, Diamond SM, Stoltenborg JK. 1996. αvβ3 integrin is not expressed uniformly throughout the vasculature: a survey of several species. Circulation 94:I 517(abstract).

De Meyer GRY, Bult H, Van Hoydonck A, Jordaens FH, Buyssens N, Herman AG. 1991. Neointima formation impairs endothelial muscarinic receptors while enhancing prostacyclin mediated responses in the rabbit carotid artery. Circ Res 68:1669–1680.

De Meyer GRY, Van Put DJM, Kockx MM, Van Schil, Bosmans R, Bult H, Buyssens N, Vannmaele R, Herman AG. 1997. Possible mechanisms of collar-induced intimal thickening. Arterioscler Thromb Vasc Biol 17:1924–1930.

Friedlander M, Brooks PC, Shaffer RW, Kincaid CM, Varner JA, Cheresh DA. 1995. Definition of two angiogenic pathways by distinct αv integrins. Science 270:1500–1502.

Giachelli CM, Bae N, Almeida M, Denhardt D, Alpers CE, Schwartz SM. 1993. Osteopontin expression is elevated during neointimal formation in rat arteries and in human atherosclerotic plaques. J Clin Invest 92:1686–1696.

Giachelli CM, Liaw L, Murry CE, Schwartz SM, Almeida M. 1995. Osteopontin expression in cardiovascular diseases. Ann NY Acad Sci 760:109–126.

Graf K, Meehan WP, Chen JZ, Law RE, Fleck E, Hsueh WA. 1996. Upregulation of αv, β3 and β5-integrin mRNA during neointima formation in the rat aorta after balloon injury. Circulation 94:I-41(abstract).

Hirota S, Imakita M, Kohri K, Ito A, Morii E, Adachi S, Kim H, Kitamura Y, Yutani C, Nomura S. 1993. Expression of osteopontin messenger RNA by macrophages in atheroslcerotic plaques. Am J Pathol 143:1003–1008.

Hoshiga M, Alpers CE, Smith LL, Giachelli CM, Schwartz SM. 1995. αvβ3 integrin expression in normal and atherosclerotic artery. Circ Res 77:1129–1135.

Ip JH, Fuster V, Badimon L, Badimon J, Taubman MB, Chesebro JH. 1990. Syndromes of accelerated atherosclerosis: role of vascular injury and smooth muscle cell proliferation. J Am Coll Cardiol 15:1667–1687.

Janat MF, Argraves WS, Liau G. 1992. Regulation of vascular smooth muscle cell integrin expression by transforming growth factor β1 and by platelet-derived growth factor-BB. J Cell Physiol 151:588–595.

Jawien A, Bowen-Pope DF, Lindner V, Schwartz SM, Clowes AW. 1992. Platelet-derived growth factor promotes smooth muscle migration and intimal thickening in a rat model of balloon angioplasty. J Clin Invest 89:507–511.

Jones JI, Prevette T, Gockerman A, Clemmons DR. 1996. Ligand occupancy of the αvβ3 integrin is necessary for smooth muscle cells to migrate in response to insulin-like growth factor I. Proc Natl Acad Sci USA 93:2482–2487.

Kiefer MC, Bauer DM, Barr PJ. 1989. The cDNA and derived amino acid sequence for human osteopontin. Nucleic Acid Res 17:3306.

Kockx MM, De Meyer GRY, Jacob WA, Bult H, Herman AG. 1992. Triphasic sequence of neointimal formation in the cuffed carotid artery of the rabbit: Arterioslcer Thromb 12:1447–1457.

Kockx MM, De Meyer GRY, Andries LJ, Bult H, Jacob WA, Herman AG. 1993. The endothelium during cuff-induced neointima formation in the rabbit carotid artery. Arterioscler Thromb 13:1874–1884.

Le Breton H, Rabbani R, Plow EF, Mousa SA, Lincoff AM, Forudi F, Topol EJ. 1996. The role of integrins αIIbβ3 (glycoprotein IIb/IIIa) and αvβ3 (the vitronectin receptor) in a guinea pig model of restenosis. Circulation 94:I-517(abstract).

Liaw L, Skinner MP, Raines EW, Ross R, Cheresh DA, Schwartz SM. 1995a. The adhesive and migratory effects of osteopontin are mediated via distinct cell surface integrins: role of αvβ3 in smooth muscle cell migration to osteopontin in vitro. J Clin Invest 95:713–724.

Liaw L, Lindner V, Schwartz SM, Chambers AF, Giachelli CM. 1995b. Osteopontin and β3 integrin are coordinately expressed in regenerating endothelium in vivo and stimulate Arg-Gly-Asp-dependent endothelial migration in vitro. Circ Res 77:665–672.

Liaw L, Lombardi DM, Almeida MM, Schwartz SM, deBlois D, Giachelli CM. 1997. Neutralizing antibodies directed against osteopontin inhibit rat carotid neointimal thickening after endothelial denudation. Arterioscler Thromb Vasc Biol 17:188–193.

Lincoff AM, Tcheng JE, Ellis SG, Moliterno DJ, Kitt MM, Debowey D, Topol EJ. 1995. Randomized trial of platelet glycoprotein IIb/IIIa inhibition with integrelin for prevention of restenosis following coronary intervention. The IMPACT-Angiographic substudy. Circulation 92: I607(abstract).

Lindner V, Majack RA, Reidy MA. 1990. Basic fibroblast growth factor stimulates endothelial regrowth and proliferation in denuded arteries. J Clin Invest 85:2004–2008.

Liu MW, Roubin GS, King SB III. 1989. Restenosis after coronary angioplasty: potential biological determinants and role of intimal hyperplasia. Circulation 79:1374–1387.

Lopez CA, Hoyer JR, Wilson PD, Waterhouse P, Denhardt DT. 1993. Heterogeneity of osteopontin expresssion among nephrons in mouse kidneys and enhanced expression in sclerotic glomeruli. Lab Invest 69:355–363.

Matsuno H, Stassen JM, Vermylen J, Deckmyn H. 1994. Inhibition of integrin function by a cyclic RGD-containing peptide prevents neointima formation. Circulation 90:2203–2206.

Nobuyoshi M, Kimura T, Nosaka H, Mioka S, Ueno K, Yokoi H, Hamsaki N, Horiuchi H, Ohishi H. 1988. Restenosis after successful percutaneous transluminal coronary angioplasty: serial angiographic follow-up of 229 patients. J Am Coll Cardiol 12:616–623.

O'Brien ER, Garvin MR, Stewart DK, Hinohara T, Simpson JB, Schwartz SM, Giachelli CM. 1994. Osteopontin is synthesized by macrophage, smooth muscle and endothelial cells in primary and restenotic human coronary atherosclerotic plaques. Arterioscler Thromb 14:1648–1656.

Rabb H, Barroso-Vicens E, Adams R, Pow-Sang J, Ramirez G. 1996. AlphaV/Beta3 and AlphaV/Beta5 integrin distribution in neoplastic kidney. Amer J Nephrol 16:402–408.

Serruys PW, Luiten HE, Beatt KJ, Geuskens R, De Feyter PJ, Van den Brand M, Reiber JHC, Ten Katen HJ, van Es GA, Hugenholtz PG. 1988. Incidence of restenosis after successful coronary angioplasty: a time-related phenomenon. A quantitative angiographic study in 342 consecutive patients at 1, 2, 3, and 4 months. Circulation 77:361–371.

Shanahan CS, Weissberg PL, Metcalfe JC. 1993. Isolation of gene markers of differentiated and proliferating vascular smooth muscle cells. Circ Res 73:193–204.

Smith JW, Vestal DJ, Irwin SV, Burke TA, Cheresh DA. 1990. Purification and functional characterization of integrin αvβ5: An adhesion receptor for vitronectin. J Biol Chem 265:11008–11013.

Srivatsa SS, Fitzpatrick LA, Tsao PW, Reilly TM, Holmes DR Jr, Schwartz RS, Mousa SA. 1997. Selective αvβ3 integrin blockade potently limits neointimal hyperplasia and lumen stenosis following deep coronary arterial stent injury: Evidence for the functional importance of integrin αvβ3 and osteopontin expression during neointima formation. Cardiovasc Res 36:408–428.

Tezuka K, Sato T, Kamioka H, Nijweide PJ, Tanaka K, Matsuo T, Ohta M, Kurihara N, Hakeda Y, Kumegawa M. 1992. Identification of osteopontin in isolated rabbit osteoclasts. Biochem Biophys Res Commun 186:911–917.

Topol EJ, Califf RM, Weisman HF, et al. on behalf of the EPIC investigators. 1994. Randomized trial of coronary intervention with antibody against platelet IIb/IIIa integrin for reduction of clinical restenosis: results at six months. Lancet 343:881–886.

Walton H, Corjay MH, Diamond SM, Kearney M, Strzemienski P, Solomon K, Mousa SA, Reilly TR. 1996. Evaluation of monoclonal antibodies against the integrin receptor αvβ3. FASEB 10:A692(abstract).

Wilcox JN. 1993. Fundamental principles of in situ hybridization. J Histochem Cytochem 41:1725–1733.